ISBN: 978-3-95450-209-7 ISSN: 2226-0358 doi:10.18429/JACoW-ICALEPCS2019-MOPHA114

ACHIEVING OPTIMAL CONTROL OF LLRF CONTROL SYSTEM WITH ARTIFICIAL INTELLIGENCE *

R. Pirayesh
Department of Mechanical Engineering, University of New Mexico, Albuquerque, NM, USA
J. A. Diaz Cruz, S. G. Biedron[1], M. Martinez-Ramon, S. I. Sosa
Department of Electrical and Computing Engineering,
University of New Mexico, Albuquerque, NM, USA
[1] also at Department of Mechanical Engineering,
University of New Mexico, Albuquerque, NM, USA

Abstract

Microphonics and Lorentz Force Detuning are common sources of detuning in Superconducting Radio-Frequency (SRF) cavities and continuous wave (CW) systems. Requirements as tight as 10 Hz, are common in such systems and are equivalent to change in cavity length of only a few nanometers. Traditional approaches to mitigate detuning in SRF cavities consist of mechanical modifications of the cavity/cryomodule environment and advance control techniques such as active compensation. In this research, we explore Artificial Intelligence (AI) techniques that can improve existing control systems to ensure better performance and lower detuning. Machine learning (ML), as part of AI, can learn the complexity and non-linear behaviour of the system. Deep Learning (DL), as one of the greatest algorithms in ML, can scale and distribute well on the cores of high-performance computers (HPC). This enables the controller to learn the huge amount of data coming from diagnostic instrumentation. Furthermore, Gaussian Process (GP) can be used in parallel with DL to increase the performance of ML. We describe such AI implementation on a computer model of the RF control of an SRF cavity for LCLS-II. This model, called Cryomodule-on-Chip (*CMOC*), was developed at LBNL. It is our main goal to implement such AI-supported control for the compensation of microphonics in LCLS-II SRF cavities.

INTRODUCTION

The quality of the electron beam affects the quality of the X-rays produced in Free Electron Lasers. The amplitude and phase of the electromagnetic fields in accelerating cavities are controlled by the Low Level RF (LLRF) control system. In particular, for the Linac Coherent Light Source upgrade (LCLS-II), the LLRF must provide high stability of the phase and amplitude to produce narrow-band hard X-rays [1].

In this contribution, we investigate the use of AI as a tool to enhance the stability of the LLRF system. We utilize *CMOC*, a software developed at LBNL, to model the different noises present in the system; later on *CMOC* is also used to model the LLRF. AI and ML have been previously used in conjunction with control systems for numerous applications: We utilized formation flying control systems to keep two satellites in formation [2–4]. We also used different AI frameworks to enhance the performance of the control [5–7], similar approaches can be implemented for the control of particle accelerators and their sub-components, e.g. the LLRF. We have previously explained the challenges of applying these AI techniques to LLRF [8].

* The study at the University of New Mexico was supported by DOE Contract DE-SC0019468

LCLS-II AND LLRF MODEL

LCLS-II is composed of 35 cryomodules, each with 8 SRF cavities used for staged acceleration of an electron beam. The RF power driving each of these 280 accelerating cavities is provided by Solid State Amplifiers (SSA) [9] and controlled by the LLRF. The current LLRF framework is a proportional and integral (PI) controller that is implemented in an FPGA [10] and is sketched in Fig. 1.

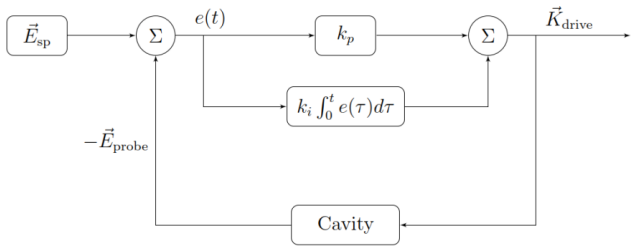

Figure 1: Diagram of a PI Controller.

The chosen gains for this PI controller are k_p = 1200 and k_i = 3.8×10^7 [11]. These gains can further be tuned dynamically with ML algorithms, according to the cavity probe signal, forward power, reverse power, and other system parameters, e.g. minimizing reflected power and losses. As a result, the gain coefficients will take values from a set of optimal parameters that minimize errors depending un the particular state of the system.

Cavity Model

A model of the system encompassing the SRF cavity, the LLRF, and the cryomodule was developed by the LLRF team at LBNL and has been used to study the electrodynamic performance of the system. For a cavity with several electromagnetic modes, each mode can be represented by a resonant circuit model, see Fig. 2.

ISBN: 978-3-95450-209-7 ISSN: 2226-0358 doi:10.18429/JACoW-ICALEPCS2019-MOPHA114

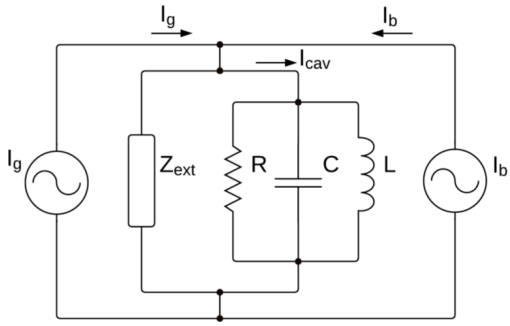

Figure 2: Circuit model of a resonant mode in a cavity.

The equations describing the electrodynamics of the system [10] are:

$$V = Se^{j\theta}, \tag{1}$$

$$\frac{d\theta}{dt} = w_d, \tag{2}$$

$$\frac{dS}{dt} = -w_f S + w_f e^{-j\theta}(2K_g\sqrt{R_g} - R_b I), \tag{3}$$

The V measures the energy stored in each mode, S and θ represent the magnitude and phase of V, respectively, w_d shows the detuning frequency, w_f shows the cavity bandwidth, K_g represents the incident wave amplitude, R_g is the coupling impedance of the beam, and I represents the beam current.

SIMULATIONS

CMOC code is used to simulate the cavity responses to the control system and different measurement noises. Figure 3 represents the cavity field amplitude versus time when the controller is not applied, and beam gets activated. Figure 4 represents the response of the control system when the feed forward control is activated. It is clear how the control system is able to keep the cavity field amplitude in the specified limits. Figure 5 represents the cavity field amplitude when there is detuning in the cavity, and still the response lies in the limits with feed-forward control activated. Figure 6 shows the response when measurement noise is applied. LLRF amplifies higher noises and it will be send back to SSA. Figure 7 represents how measurement noise in the range of 130 to 260 dBc/Hz can lead to amplitude error [11]. Noise is amplified with higher gains, and also higher noise lead to higher errors in the control system. Later on, this and other data will be passed through a ML algorithm to increase the performance of the control system.

AI FOR IMPROVED CONTROL

The methods of AI can explore the underlying complexity of a system, its behaviour, and later use that information to tune the characteristics and the parameters of the system. In this work, the complexity of the LLRF is the set of variables in the whole control system, the parameters to be tuned are the control parameters, and the control system should act optimally. Particle accelerators and their sub-components

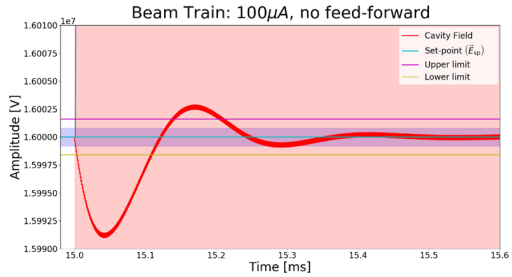

Figure 3: Beam loading noise without feed-forward.

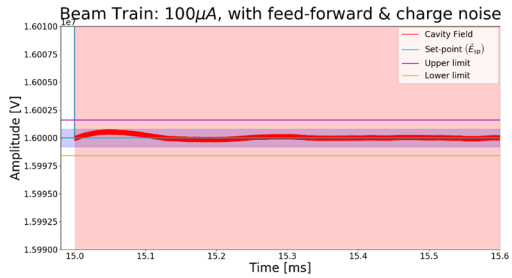

Figure 4: Beam loading noise with feed-forward.

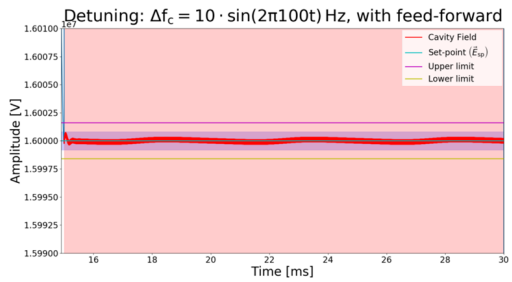

Figure 5: Detuning with feed-forward.

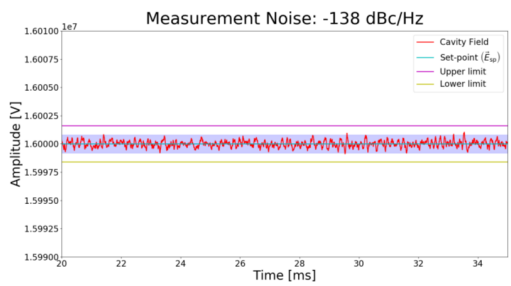

Figure 6: Measurement noise.

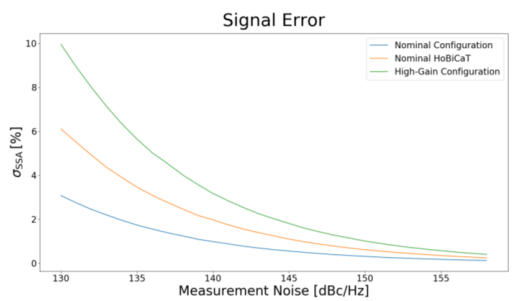

Figure 7: Signal error under different levels of measurement noise and gain configurations.

ISBN: 978-3-95450-209-7 ISSN: 2226-0358 doi:10.18429/JACoW-ICALEPCS2019-MOPHA114

are complex systems with numerous variables and phenomena happening at various time-scales. For the LLRF, the variables in the control system defining its complexity are the signal coming out of the cavity, the signals rate of change, the detuning, error of the stability, the energy spent from the RF source, PI controller parameters, and the controller settling time. The optimal state of operation is imposed as a constraint to the control system, ensuring the LLRF performance increases with the help of AI. The AI algorithm includes an optimization phase to produce the data and a ML phase to map the space of data to the whole space working environment. Figure 8 illustrates the AI approach we are investigating.

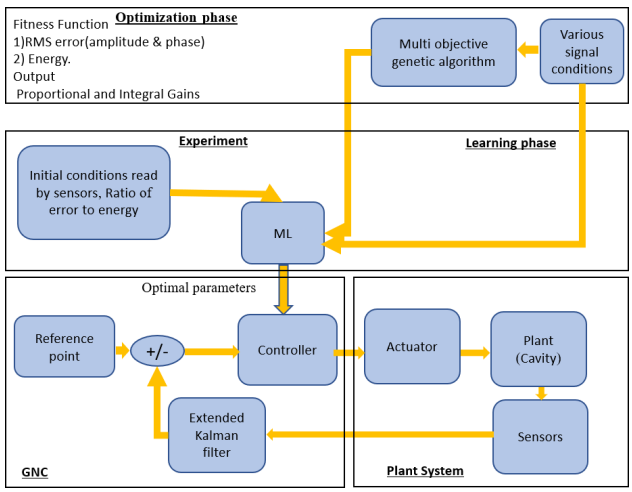

Figure 8: Our artificial intelligence framework.

To embed the constraint of finding an optimal state on the LLRF control system, an optimization algorithm finds the best possible variables that minimize a loss function. The loss functions are the RMS error and the energy spent by the system. When the loss function is minimized, they make a Pareto Front figure showing the relationship between the error and energy. Pareto Front plots the objective functions against each other. More energy can reduce the error and vice versa. We showed this trend in [5–7]. The variables in the optimization algorithm are the parameters of the controller. In this sense, for each value of the signal, the optimization algorithm finds the optimal value of the controllers parameters. In this phase, sufficient data needs to be produced so that the ML algorithm can extend the optimal state constraint into an arbitrary set of data. Figure 9 shows how the data is produced with the optimization and control system.

After sufficient data has been produced, the data is now analysed. In this step it is useful to plot each parameter against each other to see the distribution of the data. Different metrics can then be implemented to test the data quality. Interaction plot and histogram are used to measure the data distribution. Next, the data size is reduced to decrease noise and error, complexity and quantity. Principal Component Analysis (PCA) and feature selection are used to reduce the

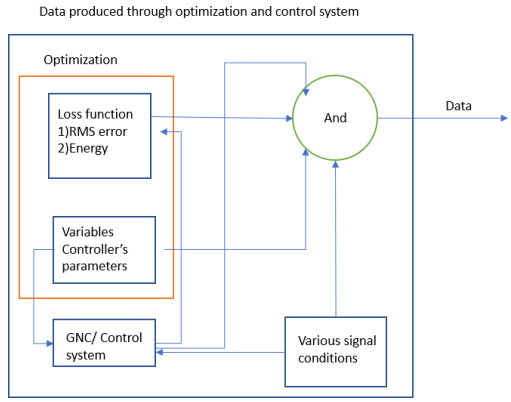

Figure 9: Data production through optimization and the control system.

features of data, which leads to maximizing the information coded in the data while reducing the computation time during the training stage. Subsequent metrics can be implemented to check for improvements on data quality with each reduction. This process repeats itself until we reach a satisfying point for the quality of data. Only then is the data fed into the ML algorithms. Figure 10 shows how the data is processed for the ML algorithms.

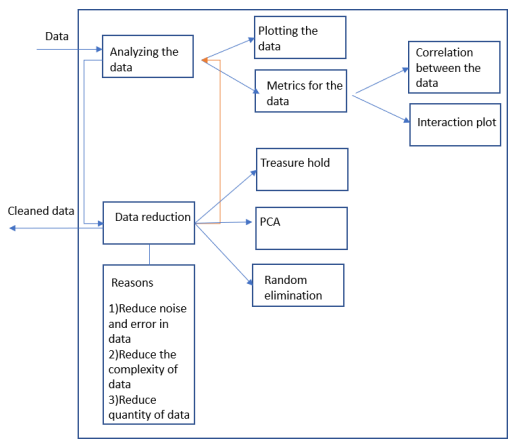

Figure 10: Data processing framework.

The input to the ML algorithm is the signal and error. The ML mechanism branches in two: Gaussian Process and Deep Learning, see Fig. 11. The first algorithm estimates the energy with confidence interval to measure the uncertainty of the estimation of the second algorithm. The second algorithm estimates the parameters of the controller, which are obtained through optimization in the AI algorithm for training. The raw data in general does not have the required format for either GP or DL and needs to be processed. Figure 12 represents the data processing for the DL in more details.

The data information can then be shown to see how it is distributed. Next, the non-valued data is removed. The resulting data set can now be separated into testing and training sub-sets. After that, the input and output to the DL is assigned and we can look at statistical parameters, like

ISBN: 978-3-95450-209-7 ISSN: 2226-0358 doi:10.18429/JACoW-ICALEPCS2019-MOPHA114

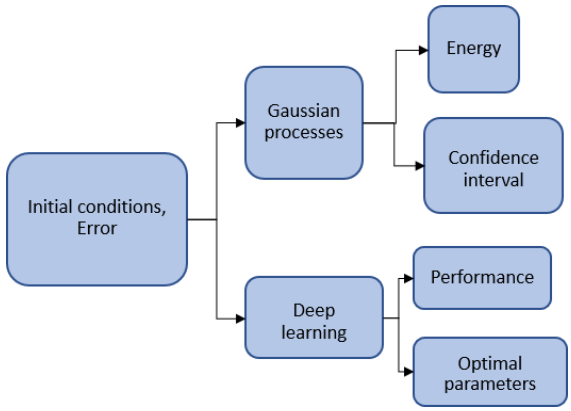

Figure 11: Deep Learning and Gaussian Process learning.

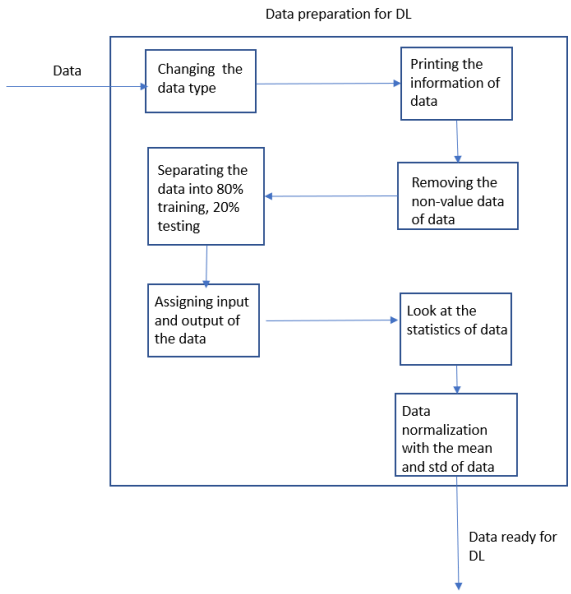

Figure 12: Data process for the deep learning.

the mean and the standard derivation. The mean and the standard deviation of the training set are in such a way as to normalize the input to the DL; the DL output, however, is not normalized. Figure 13 shows the algorithm used in the DL framework. This will be implemented and processed on High Performance Computer (HPC) resources.

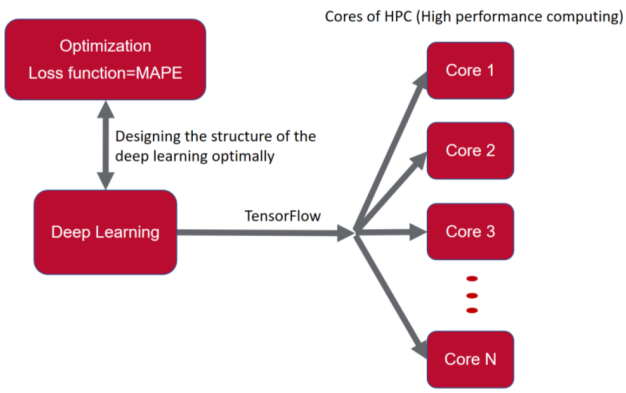

Figure 13: Deep learning architecture.

The data enters the DL algorithm that minimizes the mean square error (MSE) and mean absolute percentage error (MAPE). The whole process runs on an HPC, using *TensorFlow* to distribute the neurons on the multiple cores to be used. Figure 14 represents the optimization loops used in the deep learning algorithm.

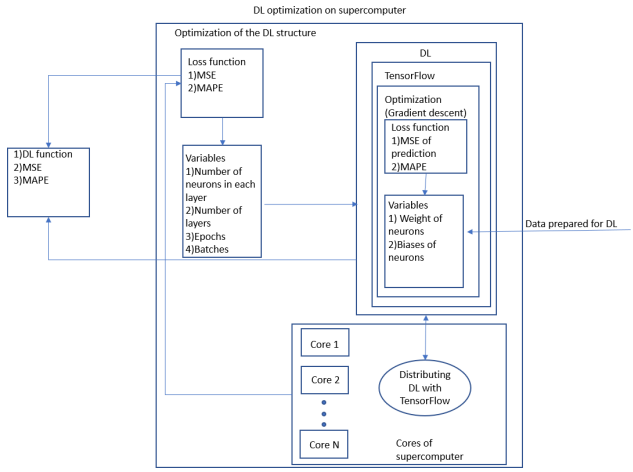

Figure 14: Deep learning optimization algorithm.

The hyperparameters are introduced as variables in the first loop of optimization for the deep learning. The optimization algorithm is gradient descent in the second loop. The chosen loss function, either MSE or MAPE, is minimized in the first loop as well to find the optimal number of layers and neurons for the deep learning architecture.

SUMMARY AND FUTURE WORK

The performance of the existing LLRF control system for SRF cavities in LCLS-II, which is a PI controller, can further benefit from AI algorithms. An AI algorithm can be used to select the optimal values of the P and I gains based on the working condition, characterised by live readouts coming out of the LLRF control system. In particular, Gaussian Process and Deep Learning are two ML algorithms that can learn the working condition of the LLRF and predict an optimal controller configuration for the LLRF. This technology has the potential of compensating in real-time for cavity detuning arising from microphonics and Lorentz Force Detuning, yielding in turn a higher stable electron beam and higher-quality X-rays. This is on-going work, we will use HPC systems to perform the DL training of *CMOC* simulated data and plan to test this AI-upgraded controller into LCLS-II test cavities.

ACKNOWLEDGEMENTS

We are very thankful to our collegues from the LCLS-II LLRF group: Larry Doolittle, Gang Huang and Carlos Serrano from LBNL, Andrew Benwell and Alex Ratti from SLAC. We are also thankful to *Element Aero* and Argonne Leadership Computing Facility for facilitating computing resources.

ISBN: 978-3-95450-209-7 ISSN: 2226-0358 doi:10.18429/JACoW-ICALEPCS2019-MOPHA114

REFERENCES

[1] Performance and Functional requirements for the LCLS-II Low Level RF System. LCLSII-2.7-FR-0371-R0

[2] A. Naseri *et al.*, "Formation Flying of a Two-CubeSat Virtual Telescope in a Highly Elliptical Orbit," *2018 SpaceOps Conference*, 2018. doi:10.2514/6.2018-2633

[3] R. Pirayesh *et al.*, "Attitude Control of a Two-CubeSat Virtual Telescope in Highly Elliptical Orbits," *2018 AIAA Guidance, Navigation, and Control Conference*, 2018. doi:10.2514/6.2018-0866

[4] R. Pirayesh *et al.*, Hybrid Attitude Control of a Two-CubeSat Virtual Telescope in a Highly Elliptical Orbit," 2017, presentation only.

[5] R. Pirayesh, A. Naseri, F. Moreu, S. Stochaj, N. Shah, and J. Krizmanic, "Attitude Control Optimization of a Two-CubeSat Virtual Telescope in a Highly Elliptical Orbit," in *Space Operations: Inspiring Humankind's Future*, pp. 233-258, 2019. Springer, Cham. doi:10.1007/978-3-030-11536-4_11

[6] R. Pirayesh *et al.*, "Deep learning and Gaussian process approach for optimal attitude control of a Two-CubeSat Virtual Telescope,", *Small Satellite Conference SSC19*, 2019, poster SSC19-WP2-24.

[7] R. Pirayesh *et al.*, "Attitude Control Optimization of a Virtual Telescope for X-ray Observations," *Small Satellite Conference SSC18*, 2018, p. SSC18-WKIV-05.

[8] J. A. Diaz Cruz, S. Biedron, M. Martinez-Ramon, S. I. Sosa Guitron, and R. Pirayesh, "Studies in Applying Machine Learning to Resonance Control in Superconducting RF Cavities", in *Proc. NAPAC'19*, Lansing, MI, USA, Sep. 2019. doi:10.18429/JACoW-NAC2019-WEPLM01 to be published.

[9] L. R. Doolittled *et al.*, "LLRF Control of High Q_L Cavities for the LCLS-II", in *Proc. IPAC'16*, Busan, Korea, May 2016, pp. 2765–2767. doi:10.18429/JACoW-IPAC2016-WEPOR042

[10] *LCLS-II System Simulations: Physics*, LBNL LLRF Team, Oct. 2015.

[11] C. Serrrano, L. Doolittle, and C. Rivetta, "Modeling & Simulations," LCLS-II LLRF Review, Mar. 2016.